Taylor & Francis
Taylor & Francis Group

Journal of Toxicology and Environmental Health, Part A
Current Issues

ISSN: 1528-7394 (Print) 1087-2620 (Online) Journal homepage: https://www.tandfonline.com/loi/uteh20

Toward a Better Understanding of Pesticide Dermal Absorption: Diffusion Model Analysis of Parathion Absorption *in Vitro* and *in Vivo*

Matthew A. Miller & Gerald B. Kasting

To cite this article: Matthew A. Miller & Gerald B. Kasting (2009) Toward a Better Understanding of Pesticide Dermal Absorption: Diffusion Model Analysis of Parathion Absorption *in Vitro* and *in Vivo* , Journal of Toxicology and Environmental Health, Part A, 73:4, 284-300, DOI: 10.1080/15287390903249230

To link to this article: https://doi.org/10.1080/15287390903249230

Journal of Toxicology and Environmental Health, Part A, 73:284–300, 2010

ISSN: 1528-7394 print / 1087-2620 online
DOI: 10.1080/15287390903249230

Taylor & Francis
Taylor & Francis Group

TOWARD A BETTER UNDERSTANDING OF PESTICIDE DERMAL ABSORPTION: DIFFUSION MODEL ANALYSIS OF PARATHION ABSORPTION *IN VITRO* AND *IN VIVO*

Matthew A. Miller, Gerald B. Kasting

James L. Winkle College of Pharmacy, University of Cincinnati Academic Health Center, Cincinnati, Ohio, USA

Human skin absorption of radiolabeled parathion was studied *in vitro* at specific doses (mass loadings) of 0.4, 4.0, 41, or 117 μg/cm^2, with and without occlusion. The compound was applied in small volumes of acetone solution to split-thickness skin. Permeation of radiolabel into the receptor solutions was monitored for 76 h, after which the tissue was dissected and analyzed for residual radioactivity. For the 3 lower doses, cumulative permeation after 76 h was approximately dose-proportional, ranging from 28.5–30.5% of applied dose (unoccluded) to 45.5–55.7% (occluded). Total absorption, calculated as receptor fluid plus dermis content, followed a similar pattern. Both permeation rate and total absorption continued to increase up to the highest dose tested, consistent with results from other laboratories. These results are compared with predictions from a previously developed skin diffusion model (Kasting et al., 2008a). The model predicted total absorption to within a factor of 1.4 at 0.4 μg/cm^2 and 1.6 at 4 μg/cm^2, but substantially underpredicted absorption at the 2 higher doses. The analysis showed that parathion partitioned more favorably into the stratum corneum than the diffusion model prediction. Nevertheless, comparison of the model predictions to a previously reported human study showed that the skin absorption model, when corrected for surface losses occurring *in vivo*, satisfactorily described *in vivo* dermal absorption of parathion applied at 4 μg/cm^2 to various body sites.

The skin absorption of parathion (*O,O*-diethyl-*O*-4-nitrophenyl phosphorothioate, CAS number 56-38-2) has been extensively studied in humans (Maibach et al., 1971; Feldmann & Maibach, 1974; Maibach & Feldmann, 1974) and a variety of other species *in vivo* (Bucks et al., 1990; Qiao et al., 1993, 1994; Qiao & Riviere, 1995; Reifenrath & Hawkins, 1986; Reifenrath et al., 1991; Shah & Guthrie, 1983; Van der Merwe et al., 2006) and *in vitro* (Bartek & LaBudde, 1975; Chang & Riviere, 1991, 1993; Chang et al., 1994; Hawkins & Reifenrath, 1984; Moody et al., 2007; Reifenrath, 1995; Reifenrath & Hawkins, 1986; Reifenrath et al., 1991; van der Merwe & Riviere, 2005). Parathion is of interest not only as a pesticide, but also as a surrogate for organophosphorus nerve agents (Moody et al., 2007; Wester et al., 2000). These results were recently reviewed in this journal in the context of new *in vitro* absorption measurements made by Moody and coworkers (2007). This highly lipophilic pesticide penetrates skin well, occasional low *in vitro* permeation results notwithstanding (Hawkins & Reifenrath, 1984). The Reifenrath et al. (1991) assessment that these low values were due to poor clearance from full-thickness dermis is in accord with current thinking about methodology for studying skin absorption of highly lipophilic compounds (OECD, 2004). Most *in vitro* studies overpredict human *in vivo* absorption of parathion

Received 3 May 2009; accepted 10 August 2009.
Address correspondence to Gerald B. Kasting, James L. Winkle College of Pharmacy, University of Cincinnati Academic Health Center, PO Box 670004, Cincinnati, OH 45267-0004, USA. E-mail: Gerald.Kasting@uc.edu

from the volar forearm (Maibach et al., 1971; Feldmann & Maibach, 1974), but not that from many other body sites (Maibach et al., 1971). The factors leading to these differences are not completely understood.

The needs remain to reconcile the various experimental measurements of parathion skin absorption and to extrapolate these laboriously obtained results to other chemicals and exposure conditions. Mathematical models provide a means to this end. A systemic pharmacokinetic model for topical and intravenous administration of parathion to pigs was developed that provided a framework for the cutaneous and systemic metabolism of this compound (Qiao & Riviere, 1995; Qiao et al., 1994). More recently, the same group presented a physiologically based pharmacokinetic (PBPK) model for dermal absorption of three organophosphorus pesticides including parathion through porcine skin *in vitro* that included details of stratum corneum (SC) structure relevant to a presumed tortuous lipid absorption pathway (Van der Merwe et al., 2006). A drawback of this model is that some parameters, e.g., the mass transfer factor MTf, were estimated from data without a theoretical basis. The model has not, to our knowledge, been successfully applied to predict or interpret human skin absorption. A diffusion/evaporation model was developed for chemical disposition on skin based on detailed SC (Nitsche et al., 2006; Wang et al., 2006, 2007) and dermis (Kretsos & Kasting, 2007; Kretsos et al., 2008) microstructure that shows promise for predicting pesticide absorption (Bhatt et al., 2008; Kasting et al., 2008a); however, its use to date has been largely confined to analyzing *in vitro* skin absorption studies. In this report a new *in vitro* human skin permeation study with parathion designed to test the dose dependence and effect of occlusion on absorption is presented. The results are compared with those obtained in other laboratories (Chang & Riviere, 1993; Moody et al., 2007; Reifenrath et al., 1991) and analyzed in terms of the diffusion/evaporation model. Finally, model predictions are compared to human *in vivo* absorption of parathion applied in acetone at a dose of 4 $\mu g/cm^2$ to various body sites (Maibach et al., 1971). A case is made that the diffusion model, when run in a manner that incorporates surface losses commonly encountered in occupational exposures, satisfactorily represents the absorption rates inferred from this study.

MATERIALS AND METHODS

Materials

Parathion, [ring-^{14}C(U)] labeled (80 mCi/mmol; 0.1 mCi/ml), was purchased from American Radiolabeled Chemicals (St. Louis, MO). The radiochemical purity was stated by the manufacturer to be 99%. A specific activity this high indicates that some of the molecules were double-labeled (single-label limit is 62.3 mCi/mmol). All experiments were done within 2 mo of receiving the radiochemical. Unlabeled parathion was purchased from Sigma-Aldrich (St. Louis, MO). The purity was estimated by the manufacturer to be 98.8% by high-performance liquid chromatography (HPLC). Calcium-free Dulbecco's phosphate-buffered saline was obtained from Sigma-Aldrich (St. Louis, MO). Pesticide-grade acetone was purchased from Fisher Scientific (Pittsburgh, PA). Split-thickness human cadaver skin from the posterior torso (2 donors) and anterior leg (1 donor), having a nominal thickness of 400 μm, was procured from the New York Firefighters Skin Bank. The skin was preserved in RPMI 1640 with 10% glycerol, oxacillin sodium, and gentamicin and kept at –70°C until use.

Skin Permeation Study

Excised split-thickness human cadaver skin was mounted on modified Franz diffusion cells (Merritt & Cooper, 1984). A skin integrity test was performed with ^3H_2O as described in Kasting et al. (1994). The median cumulative amounts of ^3H_2O collected in the receptor compartment after 1 h of accepted cells in the integrity test were 0.70, 0.32, and 1.39 $\mu l/cm^2$ for the 3 donor skins, and the average value over all cells was 0.87 $\mu l/cm^2$. Cells in which greater than 2 $\mu l/cm^2$ ^3H_2O was absorbed were rejected. Test conditions were as previously

described (Bhatt et al., 2008) with the following modifications/clarifications: The receptor solution was Dulbecco's phosphate-buffered saline (pH 7.4) with 0.02% sodium azide w/v added as a preservative. The surfactant used in Bhatt et al. (2008) was not included in the receptor solution; nor was bovine serum albumin, because the water solubility of parathion is greater than 10 μg/ml, a condition that leads to acceptable *in vitro* results with saline receptor solutions (Bronaugh & Stewart, 1984; Kasting et al., 1997). The exterior of the ground glass joint holding the skin was sealed with Parafilm. Radiolabeled parathion solutions in acetone (5 μl and 0.1 μCi per 0.79-cm^2 cell) were applied to the skin following an overnight equilibration, yielding average doses of 0.4, 4, 41, or 117 μg/cm^2. Each dose was studied under occluded and unoccluded conditions, yielding a total of eight treatments. Occlusion was achieved by covering the top of the donor chamber with aluminum foil and a glass cap, which were placed over the top within 30 s after dosing and held securely with a rubber band. Under these conditions most of the acetone evaporated from the skin surface prior to application of the occlusive covering, based on measurements made in our laboratory (Ray Chaudhuri et al., 2009; R. Gajjar, personal communication). The skin was obtained from three donors with two to five replicates per donor for each treatment. Each treatment was studied on at least 10 skin samples.

Cells and the thermostatted blocks were placed in a fume hood with the sash raised to 18 inches. The entire receptor solution (4.5 ml) was collected at 2, 4, 9, 24, 32, 54, or 76 h post dose. At this point the skin was dissected to obtain epidermis and dermal samples, and the part of the skin (both epidermis and dermis) that was pressed in the ground glass joint was cut away from the rest. Each of these three portions was then dissolved separately in 2 ml Soluene. The diffusion cells were rinsed with approximately 1.5 ml acetone and the wash was collected in a separate vial. Parafilm and aluminum foil were also collected in individual vials. All samples were analyzed by liquid scintillation counting (LSC). Tissue analyses were corrected for recovery of a known dose of [^{14}C]parathion applied to control samples. The correction factors were 1.6, 1.4, and 1.2 for epidermis, dermis, and joint, respectively. Data so obtained were averaged for each treatment for each donor and then averaged across donors to obtain the reported results.

Uptake/Desorption Study

A study of the equilibrium uptake of [^{14}C]parathion from aqueous solution into isolated human SC followed by a desorption time course was conducted as described in Kasting et al. (2005). The study employed five samples of SC from one surgical skin donor prepared by heat separation followed by trypsinization. SC samples were immersed for 24 h in the same buffer solution used in the permeation studies but initially containing 6.9 μg/ml of parathion spiked with 0.17 μCi/ml of [^{14}C]parathion. The equilibrium concentrations of parathion in the uptake solution were about 2 μg/ml. Samples were then sequentially desorbed into fresh buffer solution for 4 d. The SC was then dissolved with Solvable for 2 h at 65°C. Residual levels of radioactivity in the tissue were measured. Analysis of these data according to homogeneous membrane theory (Kasting et al., 2005) allowed an independent determination of diffusivity D_{sc} and partition coefficient K_{sc} for parathion in fully hydrated human SC. In this analysis D_{sc} was determined from the linear portion of a plot of amount desorbed versus the square root of time, and K_{sc} was estimated from the ratio of desorbable radioactivity levels in the tissue to those in the uptake solution. Thus, parathion that was bound to the tissue in an irreversible or slowly reversible manner was not included in the calculation.

Data Analysis

Cumulative absorption data from all permeation experiments were analyzed using the numerical methods and diffusion/evaporation model described in Kasting et al. (2008a). A brief introduction to this model is presented in the Appendix. Physical properties of parathion relevant to this calculation were taken from the literature. Particular attention was paid to

vapor pressure, P_{vp}, which is the most important determinate of volatility from skin. Log P_{vp} values at various temperatures from different sources were plotted versus the reciprocal of absolute temperature, and the value at 32°C (skin temperature) was determined by linear regression. A linear plot is anticipated based on the Antoine equation with a constant heat of vaporization. Occluded and unoccluded skin permeation data sets were analyzed separately, but several of the parameters were shared. Each data set had 36 observations, corresponding to 7 receptor solution sampling times and 2 tissue samples (epidermis, dermis) at each of 4 doses. Parafilm and joint counts were included as amounts in the epidermis. Several model variations were considered, three of which are reported here. Model 1 employed the parameters given in Kasting et al. (2008a) with no adjustments. These calculations did not rely on the new parathion data and may thus be considered an a priori estimate or prediction. Model 2 represented an equal weighted, least-squares fit to the cumulative permeation data and tissue concentrations at all four doses in which two model parameters—stratum corneum diffusivity, D_{sc}, and stratum corneum/water partition coefficient, K_{sc}—were optimized. D_{sc} and K_{sc} were fitted separately to the data for occluded and unoccluded samples. Model 3 was similar to model 1, except that K_{sc} was optimized separately at each dose and occlusion condition. This was done to test the hypothesis that large doses of parathion increased its effective partition coefficient in the SC. In addition to the preceding descriptions, models 2 and 3 included a first-order clearance constant in the dermis, k_{de}, that accounted for binding of radiolabel to the tissue. The optimum value of k_{de} was determined to be approximately 3×10^{-5}/s independent of the model used. This parameter has the same mathematical effect as does the capillary clearance in other accounts of this model (Kasting et al., 2008a), but the interpretation of the first-order loss in this case is binding to the tissue rather than systemic uptake. An identical binding constant, $k_{ed} = k_{de}$, was assumed in the viable epidermis although the model was not sensitive to this parameter. These values were used in all the model 2 and 3 calculations. The rationale for these choices is described later.

RESULTS

Parathion Physical Properties

Physical properties relevant to the diffusion model calculation are shown in Table 1. The analysis leading to the selected value of $P_{vp} = 2.5 \times 10^{-5}$ torr at 32°C is shown in Figure 1. A least squares fit to these data yielded

$$\log P_{vp} = -4.38(1000/T) + 9.75 \qquad 293\text{K} < T < 318\text{K} \qquad n = 10; s = 0.099; r^2 = 0.95 \tag{1}$$

where P_{vp} is vapor pressure in torr and T is the temperature in Kelvin. The root mean square departure of the reported vapor pressures from Eq. (1) is 26% and the maximum deviation is 52%. Thus, it is postulated that Eq. (1) predicts parathion vapor pressure to within about 25% over the temperature range of interest for dermal studies (20-45°C).

TABLE 1. Physical and Environmental Properties of Parathion at 32°C and Standard Pressure

Parameter	Units	Value	Reference
MW	g/mol	291.26	
ρ[a]	g/cm^3	1.27[b]	ChemGold MSDS[c]
log K_{oct}[d]		3.83	EpiSuite[e]
P_{vp}[f]	torr	2.5×10^{-5} [g]	Figure 1
S_w[h]	g/L	0.011[i]	EpiSuite[e]
mp[j]	°C	6.1	EpiSuite[e]
bp[k]	°C	375	EpiSuite[e]

[a]Density.
[b]Value at 25°C.
[c]Integrated Chemical Management Solutions (2009).
[d]Octanol/water partition coefficient.
[e]U.S. EPA (2009).
[f]Vapor pressure.
[g]Estimated as described in text.
[h]Water solubility.
[i]Value at 20°C unchanged by temperature correction based on ideal solubility theory.
[j]Melting point.
[k]Boiling point.

Skin Permeation Study

The mass balance on radioactivity 76 h after application of [^{14}C]parathion to human skin *in vitro* is shown in Table 2. Cumulative permeation into the receptor solution ranged from 19 to 31% of the applied dose in unoccluded cells and from 31 to 56% in occluded cells. An appreciable amount of radioactivity was recovered from the epidermis and (for the donor that had the greatest thickness) the dermis, suggesting a long residence time of parathion in the skin layers. About 5% of the dose was trapped between the ground glass joints for all treatments. Parathion levels in the epidermis and dermis were about threefold higher in the occluded cells than the unoccluded cells for all but the highest dose, where the differences were smaller (epidermis) or nonexistent (dermis).

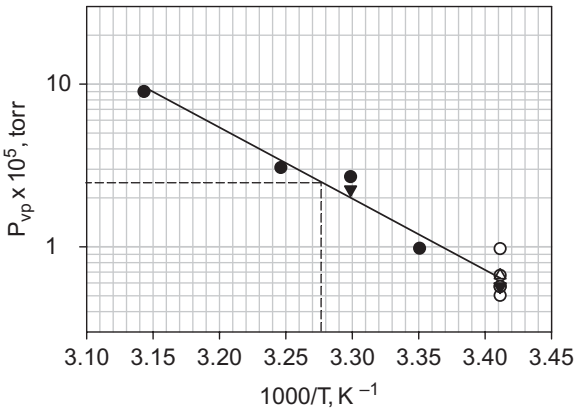

FIGURE 1. Reported vapor pressures of parathion over the temperature range 20 to 45°C: ((Kim et al., 1984); ((Agricultural Research Service, 2009); (Ngeh-Ngwainbi et al., 1986); (EpiSuite (U.S. EPA, 2009). The solid line corresponds to Eq. (1) in the text. The dashed line shows the calculated vapor pressure at 32°C.

The mean appearance of radioactivity associated with parathion in the receptor solutions as a function of time and dose is listed in Table 3. Cumulative plots of these data, expressed in micrograms per square centimeter, are shown in Figure 2. The maximum permeation rate was achieved between 4 and 24 h post dose for all treatments except for the highest dose, for which the maximum flux was reached on the second day. The permeation rate for the latter case remained fairly constant for the 3-d duration of the experiment (Figure 2, g and h). At a given dose, the cumulative permeation of parathion from occluded treatments was on average 1.7-fold higher than that for the corresponding unoccluded treatments

TABLE 2. Disposition of Radioactivity (Percent Dose) Associated With [^{14}C]Parathion 76 h After Application to Human Skin In Vitro

	Mean dose 0.4 μg/cm^2		Mean dose 4.0 μg/cm^2		Mean dose 41 μg/cm^2		Mean dose 117 μg/cm^2	
Application	Unoccluded	Occluded	Unoccluded	Occluded	Unoccluded	Occluded	Unoccluded	Occluded
In/on skin								
Foil[a]	NA	0.5 ± 0.2	NA	0.5 ± 0.1	NA	1.5 ± 0.2	NA	0.8 ± 0.2
Wash[b]	1.3 ± 0.2	5.9 ± 1.0	2.1 ± 0.4	6.8 ± 1.9	3.1 ± 0.5	9.5 ± 2.6	11.9 ± 2.5	16.1 ± 2.1
Parafilm[c]	0.0 ± 0.0	0.2 ± 0.1	0.1 ± 0.0	0.1 ± 0.0	0.2 ± 0.1	0.1 ± 0.1	0.0 ± 0.0	0.1 ± 0.0
Joint[d]	3.1 ± 0.7	8.2 ± 1.6	7.3 ± 1.5	5.7 ± 0.6	3.0 ± 1.2	6.2 ± 1.9	3.9 ± 0.2	4.8 ± 0.8
Epidermis[f]	5.7 ± 0.6	18.6 ± 2.3	4.5 ± 0.4	21.0 ± 0.5	7.7 ± 1.4	24.4 ± 1.6	20.4 ± 2.9	32.6 ± 2.8
Dermis	1.4 ± 1.1	5.0 ± 3.9	1.3 ± 0.4	4.3 ± 2.6	2.4 ± 1.1	7.5 ± 3.4	4.9 ± 3.7	4.2 ± 2.4
Absorbed								
Receptor fluid	28.5 ± 3.7	52.2 ± 9.2	30.5 ± 4.4	55.7 ± 6.4	29.6 ± 4.0	45.5 ± 4.7	19.4 ± 2.6	31.0 ± 1.8
Total absorbed	29.9 ± 4.2	57.2 ± 8.5	31.8 ± 4.1	60.0 ± 5.3	32.1 ± 4.4	53.0 ± 4.2	24.3 ± 4.9	35.2 ± 3.6
Potentially absorbed	38.8 ± 3.7	84.2 ± 6.8	43.7 ± 1.0	86.8 ± 4.7	43.9 ± 5.8	83.6 ± 2.2	48.7 ± 6.8	72.7 ± 1.3
Total recovery	40.1 ± 3.5	90.7 ± 4.9	45.8 ± 2.7	94.0 ± 3.8	46.0 ± 5.3	94.7 ± 0.6	60.6 ± 6.8	89.6 ± 3.4
Missing	59.9 ± 3.5	9.3 ± 4.9	54.2 ± 2.7	5.0 ± 3.8	53.0 ± 5.3	5.3 ± 0.6	39.4 ± 6.8	10.4 ± 3.4

Note. Values are expressed as the percent of dose applied (mean ± SE of 3 donors, n = 2–5/donor).
[a]Foil, amounts found on the occlusive foil.
[b]Wash, amounts found in washes of the Franz cell tops.
[c]Amounts found on the parafilm wrapped around the outside of the ground glass joint.
[d]Joint, amounts found in the skin that was between the ground glass joints of the Franz cell.
[e]The epidermis was separated from the dermis using forceps and dissolved with a tissue solubilizer.

TABLE 3. Appearance of Radioactivity in the Receptor Solution for the [^{14}C]Parathion Skin Disposition Study Reported in Table 2 (Mean of 3 donors, n = 2–5/Donor)

	Percent of dose						
Dose, μg/cm^2	0–2 h	2–4 h	4–9 h	9–24 h	24–32 h	32–54 h	54–76 h
Unoccluded							
0.4	0.69	1.38	4.19	9.64	4.02	5.49	3.06
4.0	0.90	1.73	4.83	10.58	4.12	5.40	2.91
40	0.45	0.96	3.21	9.28	4.26	6.77	4.70
120	0.21	0.40	1.18	4.17	2.20	5.84	5.43
Occluded							
0.4	1.02	1.65	5.58	15.11	7.17	12.36	9.33
4.0	1.28	2.16	5.86	15.73	7.24	13.11	10.31
40	0.63	1.22	3.69	11.72	6.13	11.79	10.35
120	0.63	0.88	2.23	6.87	3.43	8.52	8.47

(range 1.5–1.8). Permeation was approximately dose-proportional for the lower three doses (0.4, 4, and 41 μg/cm^2) and still increased for the highest dose (117 μg/cm^2), but at a lower rate.

Figures 2 and 3 show the calculations from skin diffusion models 1, 2, and 3. The parameters associated with each calculation are shown in Tables 4, 5, and 6. Model 1, the a priori calculation, worked best in the case of low doses. It accurately predicted overall permeation for the occluded samples (Figure 2, b and d) and underpredicted it for unoccluded samples (Figure 2, a and c). However, it overestimated the initial permeation rates in both cases. In both cases it underestimated the residual amounts of parathion in tissue at 76 h (Figure 3). At the two higher doses, model 1 significantly underestimated the permeation rates for both unoccluded and occluded skin samples (Figures 2e-2h), as well as the residual amounts in the tissue (Figure 3). The discrepancy of model 1 from the data was greatest at the 117-μg/cm^2 dose. The pattern of departure of the model predictions from the data might be understood on the basis of the interplay of dose and the capacity of the upper stratum corneum for the permeant, as shown later.

Model 2 represented a fit to the data in which parathion diffusivity D_{sc} and partition coefficient K_{sc} in the stratum corneum were allowed to vary, and the first-order loss constants k_{de} and k_{ed} in the dermis and viable epidermis were included. It can be seen from Figures 2 and 3 that this model reasonably approximated both the parathion permeation data and the tissue concentration data under all conditions tested. This was accomplished by means of a small (<2-fold) reduction in D_{sc} and a large (>30-fold) increase in K_{sc} for both occluded and unoccluded samples. The rise in K_{sc} means that the model estimates of the saturation concentration of parathion in the SC, C_{sat}, and the dose required to saturate the upper SC, M_{sat}, were increased by the same factor (cf. Appendix equations A-1 and A-2). This implies that the solubility of parathion in the SC was much higher than the model 1 prediction.

Further analysis showed that the small but systematic departure of model 2 permeation rates from the observed values for unoccluded samples (Figure 2) might be eliminated by upwardly adjusting the evaporation mass transfer coefficient k_g. The optimum fit was obtained using a k_g value of 1859 cm/h, about 2.5-fold higher than the default value for unoccluded samples of 738 cm/h. Such a change leads to a 13-fold reduction in the normalized sum of squared residuals, SSR_ν, versus the model 2 value, with little or no impact on the values of D_{sc} and K_{sc}. It is worth noting that the higher evaporation rate predicted by this fit cannot at present be justified, given the previous calibration work done on this parameter (Bhatt et al., 2008; Kasting et al., 2008a) and the vapor pressure data in Figure 1.

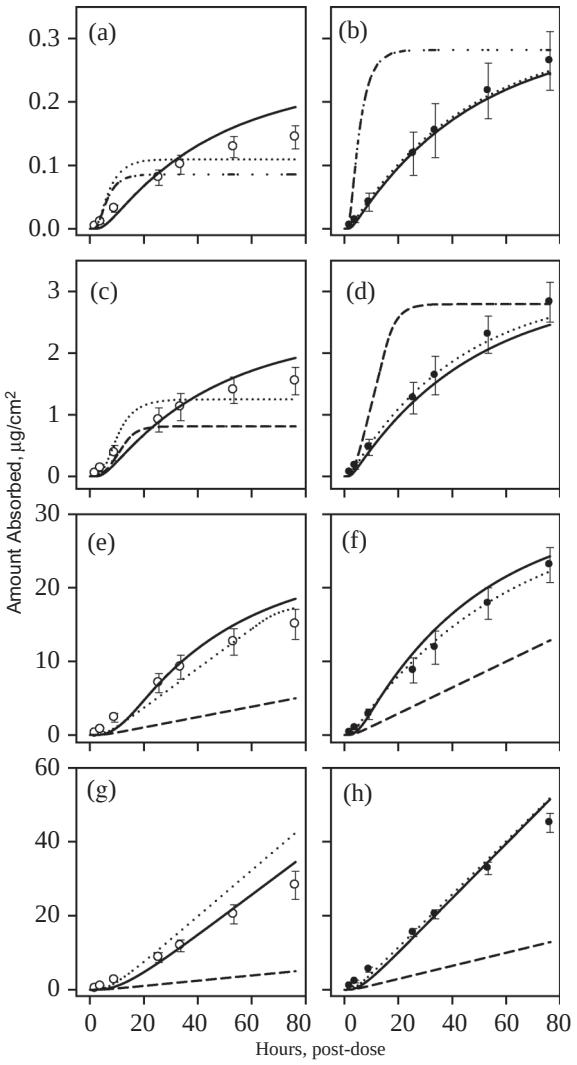

FIGURE 2. Cumulative permeation of radioactivity (mean ± SE) associated with [^{14}C]parathion through unoccluded (○) and occluded (●) human skin in vitro for the study reported in Table 2. The dashed lines represent the a priori diffusion/evaporation model (model 1). The solid lines represent a two-parameter least-squares fit to the data (model 2). The dotted lines represent a least-squares fit to the data employing the model 1 value for diffusivity (D_{sc}) and a partition coefficient (K_{sc}) that was optimized separately at each dose (model 3). (a, b) 0.4 µg/cm^2; (c, d) 4.0 µg/cm^2; (e, f) 41 µg/cm^2; (g, h) 117 µg/cm^2.

It was evident from the preceding analysis that the departures of the a priori (model 1) predictions from the experimental permeation data in Figure 2 increased with the dose applied. A scenario was considered in which parathion impacted its own permeation in a positive manner. The shape of the permeation profiles, combined with precedent from the chemical enhancer literature (Kim et al., 1992; Yamashita et al., 1993), suggested that the primary transport parameter impacted by the dose was the SC/water partition coefficient K_{sc}. Consequently a model was constructed, designated as model 3, that derived from model 1 except that a nonzero clearance constant in the dermis and viable epidermis, $k_{de} = k_{ed} = 3 \times 10^{-5}$/s, was included (as in model 2) and K_{sc} was optimized separately for each dose and occlusion condition. Results are shown in Figures 2–4. Under these constraints, K_{sc} was found to increase markedly with dose for the unoccluded samples, but not for the occluded samples (Figure 4). This analysis represents a departure from our previous treatments of chemical penetration enhancement, in which the parameter influenced by dose was D_{sc}, the diffusivity of the permeant in the SC (Kasting et al., 2008a; Miller et al., 2006). The analysis indicated that a high-quality fit could be obtained by this approach, and the K_{sc} value for the lowest dose of parathion applied to unoccluded samples approached the model 1 value.

To address the possible concern that parathion permeation and tissue concentration data in Figures 2 and 3 emphasize long exposure periods uncommon in the workplace, a plot was constructed of the cumulative permeation 9 h post dose versus the predictions from models 1 and 2 at this time. Results are shown in Figure 5. Further shown on this plot are data from Chang and Riviere (1993) showing parathion permeation through excised pig skin after 8 h. Both sets of experiments and the model calculations indicate a rapid fall in percent permeation with dose for doses greater than a threshold value that ranges from about 1 to 40 µg/cm^2. The experimental data from the present study (open and closed circles) have a higher threshold dose than do the model 1 predictions. This is reflected in the model 2 (fitted) calculation. Interestingly, model 1 matches the pig skin data (Chang & Riviere, 1993) quite closely.

Finally, a plot of model 1 and model 2 dermal absorption predictions was constructed with several removal scenarios versus urinary

TABLE 4. Model Parameters for Calculation of [^{14}C]Parathion Permeation Through Unoccluded Human Skin In Vitro

Parameter	Units	Model 1	Model 2	Model 3
Stratum corneum				
D_{sc}	$cm^2\ s^{-1}$	$[2.72 \times 10^{-11}]$[a]	1.52×10^{-11}	$[2.72 \times 10^{-11}]$
K_{sc}	—	[94.9]	3493	see Figure 5
Viable epidermis/dermis				
k_{ed}, k_{de}[b]	s^{-1}	[0]	$[3.0 \times 10^{-5}]$	3.0×10^{-5} [c]
Derived parameters				
h_{sc}^2/D_{sc}	h	18	33	18
C_{sat}	mg/cm^3	1.04	38.4	Varies
M_{sat}	$\mu g/cm^2$	0.14	5.14	Varies
k_p	cm/h	0.006	0.056	Varies
χ	—	3.69	0.18	Varies
Statistics				
n		36	36	36
s	% dose	13.9	6.7	6.1
r^2	—	—	0.57	0.68
SSR_ν[d]	$(\%\ dose)^2$	194	45	37

Note. Formulas for all parameters may be found in Bhatt et al. (2008). Parameters that do not vary between models are reported in Table 6.

[a]Brackets denote that a parameter value was fixed rather than optimized.

[b]First-order clearance constants accounting for binding of permeant to the viable tissues.

[c]Value optimized over both occluded and unoccluded data.

[d]Sum of squared residuals normalized by degrees of freedom; equivalent to χ_ν^2 in Kasting et al. (2008a).

TABLE 5. Model Parameters for Calculation of [^{14}C]Parathion Absorption Through Occluded Human Skin In Vitro

Parameter	Units	Model 1	Model 2	Model 3
Stratum corneum				
D_{sc}	$cm^2 s^{-1}$	$[7.07 \times 10^{-10}]$[a]	4.12×10^{-10}	$[7.07 \times 10^{-10}]$
K_{sc}	–	[33]	1061	see Figure 5
Viable epidermis/dermis				
k_{ed}, k_{de}[b]	s^{-1}	[0]	$[3.0 \times 10^{-5}]$	3.0×10^{-5} [c]
Derived parameters				
h_{sc}^2/D_{sc}	h	7	13	7
C_{sat}	mg/cm^3	0.37	11.67	Varies
M_{sat}	$\mu g/cm^2$	0.16	5.06	Varies
k_p	cm/h	0.016	0.074	Varies
χ	—	0.37	0.02	Varies
Statistics				
n[a]		36	36	36
s	% dose	20.5	3.6	2.0
r^2	—	—	0.96	0.99
SSR_ν[d]	$(\%\ dose)^2$	420	13	4

Note. Formulas for the transport parameters may be found in Bhatt et al. (2008). Parameters that do not vary between models are reported in Table 6.

[a]Brackets denote that a parameter value was fixed rather than optimized.

[b]First-order clearance constants accounting for binding of permeant to the viable tissues.

[c]Value optimized over both occluded and unoccluded data.

[d]Sum of squared residuals normalized by degrees of freedom; equivalent to χ_ν^2 in Kasting et al. (2008a).

TABLE 6. A Priori (Model 1) Parameters for Parathion in the Skin Diffusion Model

Parameter	Units	Unoccluded	Occluded
Stratum corneum			
D_{sc}	$cm^2\ s^{-1}$	2.7×10^{-11}	7.1×10^{-10}
K_{sc}	—	94.9	33
h_{sc}	μm	13.4	43.4
h_{dep}	μm	1.34	4.34
Viable epidermis			
D_{ed}	$cm^2\ s^{-1}$	1.08×10^{-7}	
K_{ed}	—	9.59	
h_{ed}	μm	100	
k_{ed}	s^{-1}	0	
Dermis			
D_{de}	$cm^2\ s^{-1}$	1.08×10^{-7}	
K_{de}	—	9.59	
h_{de}	μm	300	
k_{de}	s^{-1}	0[a]	
Environmental factors			
T		32	32
u	m/s	0.72	0.14
k_g	cm/h	738	207

Note. Formulas for the transport parameters may be found in Bhatt et al. (2008) or Nitsche and Kasting (2008).

[a]In vitro value. The value of k_{de} is nonzero for an in vivo simulation involving capillary clearance.

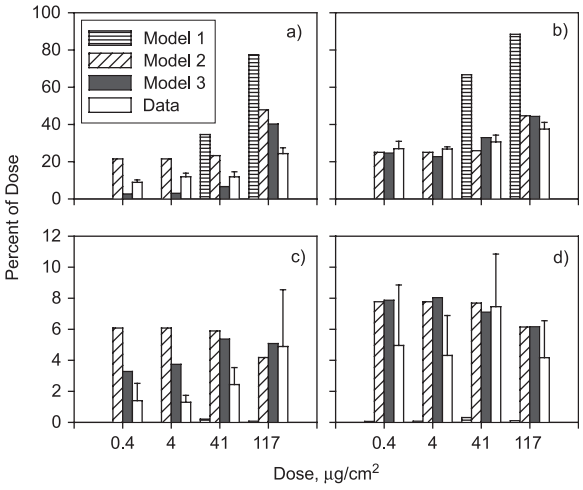

FIGURE 3. Tissue levels of parathion 76 h post dose. The experimental data from Table 2 are shown in comparison to the predictions from models 1–3. Model parameters are given in Tables 4 and 5. Missing bars reflect percent of dose values close to zero. (a) Epidermis, unoccluded; (b) epidermis, occluded; (c) dermis, unoccluded; (d) dermis, occluded.

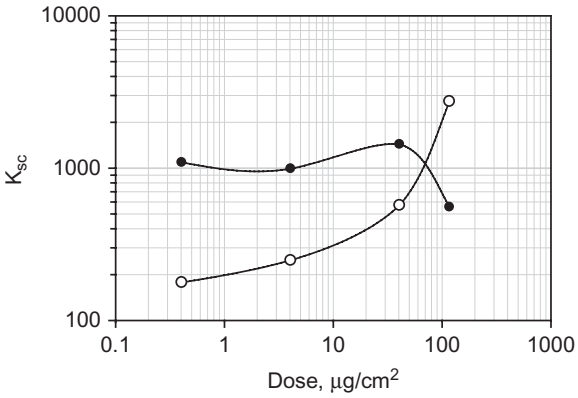

FIGURE 4. Values of SC/water partition coefficient for parathion associated with model 3, Tables 4 and 5; ○ unoccluded; ● occluded. The lines are a guide to the eye.

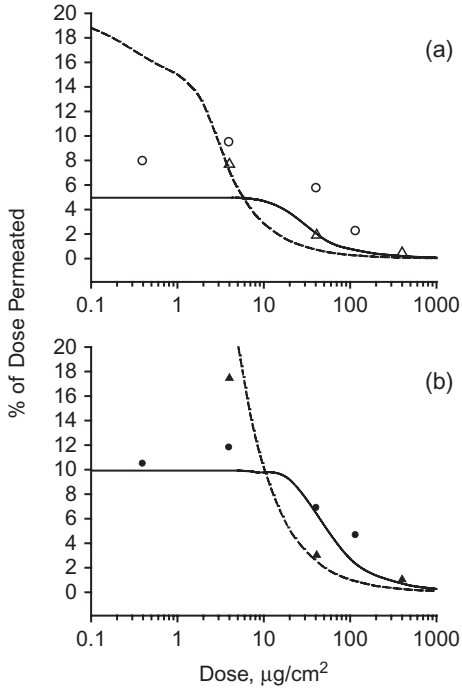

FIGURE 5. Effect of dose and occlusion on in vitro permeation of radioactivity associated with [^{14}C]parathion through human skin (circles, 9 h post dose) and pig skin (triangles, 8 h post dose): (a) unoccluded; (b) occluded. Human skin data are from the present study; pig skin data are from Chang and Riviere (1993). The dashed lines are the predictions for human skin from model 1 and the solid lines are those for model 2 (see Tables 4 and 5).

excretion rates of radioactivity following [^{14}C]parathion application at 4 μg/cm^2 to various body sites of human volunteers (Maibach et al., 1971). Results are shown in Figure 6 and discussed later.

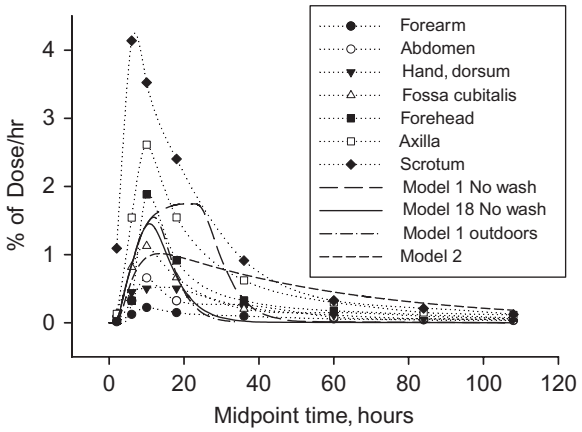

FIGURE 6. Parathion absorption rates calculated from computational model assuming a 4-μg/cm^2 dose of parathion applied in acetone (unoccluded), plotted versus urinary excretion rate of radioactivity for the same dose of [^{14}C]parathion in humans applied to various body sites (Maibach et al., 1971). The urinary excretion data were corrected for incomplete elimination as described in Feldmann and Maibach (1974). The parameters used in the calculation were those in Table 4 (models 1 and 2) with the exception of the wind velocity and wash scenario, which were varied as described in the text.

Uptake/Desorption Study

The time course for [^{14}C]parathion desorption from isolated human SC was satisfactorily described by a homogeneous membrane model (data not shown). More than 96% of the radioactivity taken up by the SC samples desorbed from the tissue in the second phase of the study. Analysis of the data (mean ± SE of 5 samples) yielded $D_{sc} = (4.1 \pm 0.9) \times 10^{-10}$ cm^2/s and $K_{sc} = 66 \pm 9$. The former value closely matched the value $D_{sc} = 4.12 \times 10^{-10}$ cm^2/s estimated from the permeation data for occluded skin (Table 5, model 2). Both of these numbers were within a factor of 2 of the a priori value of 7.07×10^{-10} cm^2/s (Table 5, model 1). On the other hand, the K_{sc} value determined from equilibrium uptake was closer to the model 1 value (33) than the model 2 value (1061). Data further reinforces the finding that transport results for organophosphorus compounds obtained or predicted from dilute aqueous solution experiments (uptake/desorption study and model 1) do not always predict the results of concentrated solutions applied to the skin (Figure 1 and model 2).

DISCUSSION

Parathion absorption through human skin appears to be a slow process, stretching over days. In a diffusion cell with no removal process other than gradual evaporation, a large proportion of the compound is eventually absorbed (Table 2); *in vivo* this is not usually the case (Maibach et al., 1971; Figure 6). A considerable amount of applied material binds to the tissue in a manner that is either irreversible or slowly reversible. These statements follow from the continuous appearance of radioactivity in the receptor solution following topical application of [^{14}C]parathion for at least 76 h (Table 3 and Figure 2) and from the appreciable tissue levels remaining after 76 h from all 4 doses (Table 2). The tissue binding is consistent with results reported by others (Moody et al., 2007). The findings also support the interpretation that SC acts like a "sink" rather than an impermeable barrier for pesticides (Wester & Maibach, 1985). The recovery of radioactivity was substantially higher for the occluded samples relative to unoccluded. Only about 5–10% of the dose remained unaccounted for in the occluded case. The additional missing material in the unoccluded samples was presumed to have evaporated from the skin.

Despite the prolonged absorption profile, lag times for absorption through skin appear to be less than 1 h for the 2 lower doses and 0.5–2.5 h for the 2 higher doses. These are consistent with the predicted lag times from models 1 and 3 (1–3 h), but lower than those from model 2 (2.3–4 h). The relatively short lag times may also reflect transport through the SC by way of a secondary pathway with a low capacity and high diffusion coefficient, such as a hair follicle. Accumulation of parathion in hair follicles was first noted by Fredriksson (1961) and may account for a significant fraction of the tissue binding of radioactivity noted in Table 2. Hair follicles are not explicitly accounted for in the present diffusion model, model 1. The inclusion of non-zero epidermis and dermis clearance constants k_{ed} and k_{de} in models 2 and 3 allowed for accumulation of

compound in the lower skin layers and may be thought of as a way of representing binding to hair follicles, albeit in a spatially averaged or distributed manner.

Occlusion Effect

Occluded cells yielded, on average, 1.7-fold higher absorption of parathion than did unoccluded cells based on either receptor fluid accumulation or total absorption (Table 2). Figure 5 shows a comparison of these data with the hydration study results of Chang and Riviere (1993) in pig skin *in vitro*. Our data fall within the range reported by these investigators, although the pattern of absorption versus dose is different. Most other studies yielded comparable hydration effects for parathion. For example, Wester et al. (2000) reported a 2.2-fold increase in skin absorption of parathion *in vitro* when dosed to wetted army uniform (1:1 nylon:cotton) as compared to dry uniform. Qiao et al. (1993) reported increases ranging from 1.7- to 5.9-fold (mean 3.2-fold) in total urinary plus fecal excretion of radioactivity associated with [^{14}C]parathion when dosed to weanling swine *in vivo* from an occluded application versus an unoccluded application. In another swine study, Qiao and Riviere (1995) reported moderately elevated dermal absorption of parathion under occlusion versus unoccluded application. However, systemic bioavailability of the parent compound was found to not rise under occlusion due to an increase in cutaneous metabolism at the occluded sites. The exception to this pattern is the 6.4-fold rise under occlusion for parathion absorption from human volar forearm *in vivo* reported by Maibach and Feldmann (1974). As Chang and Riviere (1993) noted in their study, it is possible that the aluminum foil occlusion method employed herein does not yield full hydration. However, larger hydration effects were observed for other compounds using the same diffusion cell methodology. For example, a 2- to 6-fold increase in permeation into the receptor solutions was found for tecnazene along with a 5- to 10-fold rise in total absorption (Bhatt et al., 2008). These examples show that the occlusion effect on parathion dermal absorption is about 2- to 3-fold in most cases. The higher ratio obtained by Maibach and Feldmann (1974) may have resulted from a combination of skin hydration, lower evaporation, and prevention of incidental rub-off from the occluded sites. Parathion thus follows a trend exhibited by many compounds of moderately increased skin absorption under occlusion (Zhai & Maibach, 2001).

Dose Dependence

Parathion permeation rate increased with dose up to the highest dose tested, 117 μg/cm^2 (Figure 2). The increase was approximately dose-proportional up to 41 μg/cm^2. These results are consistent with those of Moody et al. (2007), Chang and Riviere (1993), and Wester and Maibach (1985), who found increasing parathion absorption at doses up to 3200 μg/cm^2 (human skin *in vitro*), 400 μg/cm^2 (pig skin *in vitro*), and 2000 μg/cm^2 (human skin *in vivo*), respectively. They may be contrasted with the expectations from the diffusion model, which yields nearly dose-proportional permeation up to a threshold dose, M_{sat}, followed by a plateau in which total permeation is independent of dose (Kasting & Miller, 2006). In the latter region, percent absorption decreases inversely with dose—see, for example, the model 1 calculations in Figure 5. The values of M_{sat} calculated in this study for unoccluded skin were 0.14 and 5.14 μg/cm^2 for models 1 and 2, respectively (Table 4). The higher value for model 2 derives from its higher value of K_{sc}, as may be seen from Eqs. (A-1) and (A-2) in the Appendix. It is clear from Figure 2 that high doses of parathion on excised human skin are absorbed more efficiently than predicted by the a priori calculation, model 1. Although model 2 did a fairly good job of representing this absorption, a representation nearly as good was generated by model 3, in which the SC/water partition coefficient K_{sc} varied with dose. The value of K_{sc} at low, unoccluded doses approached that of model 1 (cf. Figure 4). This is consistent with the hypothesis that partially hydrated skin swells with increasing doses of organophosphorus pesticides such as parathion, an effect

not taken into account by model 1. The implication of this finding is that the model 1 predictions may still be valid for low doses of parathion applied to skin. The following example shows this to be the case.

Comparison With Clinical Data

Figure 6 shows a comparison of the absorption model calculations with [^{14}C]parathion absorption in humans as determined by the urinary excretion method of Maibach et al. (1971). The clinical protocol employed in this study was used to study absorption of a wide variety of drugs, pesticides and other chemicals (Feldmann & Maibach, 1967, 1969, 1970, 1974; Maibach et al., 1971). Although the forearm was the most common site of application, some compounds including parathion were studied on a large number of body sites (Feldmann & Maibach, 1967; Maibach et al., 1971). Data from selected sites are shown in Figure 6.

It is evident from the figure that all models shown overestimate human *in vivo* absorption rates following dosing of small amounts of parathion to the volar forearm. Equally evident is the fact that absorption from the forearm was lower than that from many other body sites; in fact, absorption from the forearm was the lowest of 13 body sites tested in the original study (Maibach et al., 1971). Absorption ratios compared to forearm ranged from 1.3 (palm) to 11.8 (scrotum). Model 1 (Table 3, unoccluded) yields a predicted cumulative absorption of parathion of 43.4% over 5 d, comparable to the 36.3% absorption measured on the forehead in the clinical study and about 5-fold higher than the forearm absorption value of 8.6%. The peak absorption rate in the calculation occurred at 22.7 h post dose, just prior to depletion of the surface parathion film. Experimental absorption rates peaked at 8–12 h post dose at most body sites (Figure 6). The calculated absorption profile using model 1 parameters can be matched to typical clinical absorption data in the Maibach et al. (1971) study either by removing the residual dose after 8 h (Figure 6, model 1, 8-h wash) or by increasing the effective wind velocity to 0.72 m/s, a representative outdoor value (Figure 6, model 1 outdoors). These artifices led to cumulative absorption over 5 d of 19.4 and 19.7%, respectively, with absorption rates peaking at 11–12 h post dose. The adjusted profiles are comparable to those obtained from the forehead and fossa cubitalis (inner crease of elbow). Cumulative absorption is just over twofold higher than the forearm value of 8.6% reported by Maibach et al. (1971) or the comparable forearm value of 9.7% reported in a later study by the same investigators (Feldmann & Maibach, 1974). Based on this analysis, it is suggested that the current absorption model (i.e., model 1 in Table 3), modified to incorporate surface loss by means of a simulated wash after 8 h, provides a reasonable estimate of parathion absorption in humans for low-to-moderate exposures. High skin exposures to parathion, i.e., doses exceeding about 40 μg/cm^2, are expected to lead to absorption rates greater than those predicted by the model, as may be seen from Figure 2. However, such exposures will not be encountered in the workplace unless there is either an accident or complete disregard for safety measures.

In Vivo/*In Vitro*/In Silico Correlations and Dermal Risk Assessment

It was stated in the introduction that most *in vitro* studies overpredict human *in vivo* absorption of parathion from the volar forearm. The present study is no exception. However, as was shown by Maibach and coworkers (1971; Figure 6), parathion absorption from other body sites is substantially higher than that from the volar forearm; thus, the majority of *in vitro* results obtained with this compound are indeed appropriate for human dermal risk assessment. Model 1 as presented herein is consistent with the *in vitro* absorption data for parathion for low, unoccluded doses (Figure 2) and thus may be considered to be appropriate for use in dermal risk assessments under these exposure conditions.

In vivo human absorption of high dermal doses of parathion and most other pesticides has not been studied. The *in vitro* results

presented here and elsewhere (Chang & Riviere, 1993; Wester & Maibach, 1985) suggest that absolute absorption rates of parathion in humans will continue to increase with loading on the skin up to very high doses, although percent absorption will decrease under these conditions. This pattern has been observed for other pesticides (Nolan et al., 1984; Wester et al., 1996) as well as for unrelated compounds (Wester & Maibach, 1976). In the case of parathion, the present diffusion model (model 1) cannot account for the increase in absolute absorption rate with dose above approximately 4 μg/cm^2. It seems likely this finding will carry over to some other compounds, although reasonable agreement of model calculations with *in vitro* absorption data for DEET (Santhanum et al., 2005) and benzyl alcohol (Miller et al., 2006) was obtained for doses several-hundred-fold higher than this value. A recent analysis of other skin absorption models (Farahmand & Maibach, 2009) suggests that they, too, often underpredicted *in vivo* absorption under high exposure conditions involving complex vehicles, in this case for drugs applied to skin in transdermal patches. The implication from both these lines of experiments is that permeation enhancing effects of topically applied compounds and/or excipients cannot be ignored when exposure levels are high. Specifically, model 1 cannot be recommended for use with organophosphorus pesticides at skin loadings above 4 μg/cm^2. Models 2 and 3 were fitted to parathion *in vitro* absorption data over a wide range of doses and do describe the *in vitro* absorption pattern over the full range of doses tested (0.4–117 μg/cm^2). However, the absorption profile calculated from model 2 comes no closer to the human *in vivo* profile than does model 1 (Figure 6). The large K_{sc} values associated with models 2 and 3 were not observed when excised SC was equilibrated with dilute aqueous solutions of parathion (uptake/desorption study). These values are specific to parathion permeation in the *in vitro* study and should not be applied to other exposure scenarios in the absence of supporting data.

SUMMARY

This study describes the absorption of parathion through human skin. In a new *in vitro* study, 19.4–30.5% of an applied dose of radiolabeled parathion in acetone was recovered in the receptor fluid of unoccluded Franz cells after 76 h. The corresponding range for occluded cells was 31–55.7%. When the amounts recovered from the dermis were included, 24.3–32.1% of the applied dose was found to be absorbed from unoccluded cells and 35.2–60% under occlusion. Permeation and total absorption increased in a dose proportional manner up to a specific dose of 41 μg/cm^2, with a further increase at 117 μg/cm^2. Absorption was described in terms of an existing skin diffusion model (model 1) and two variations thereon (models 2 and 3). The analysis showed that the *in vitro* absorption data for parathion at doses ≤4 μg/cm^2 and also excretion of radioactivity associated with a 4-μg/cm^2 dose of parathion in acetone applied to human subjects *in vivo* were satisfactorily described by model 1, although a simulated wash step was included in the latter case to better match the excretion profile. Absorption of larger doses of parathion *in vitro* was underpredicted by model 1 in a manner consistent with chemical penetration enhancement. The analysis indicated that large doses of parathion applied to unoccluded skin lead to an increase in solubility and partitioning of the compound in the stratum corneum.

We acknowledge a helpful conversation with Dr. John Kissel. Financial support for this study was provided by NIOSH/CDC grant R01 OH007529. The conclusions reached represent the opinions of the authors and have not been endorsed by NIOSH.

APPENDIX: OUTLINE OF SKIN DIFFUSION MODEL

The diffusion model employed in the present analysis has been summarized several times. The model framework and transport parameters for unoccluded skin may be found in Kasting et al. (2008a, 2008b). Additional details, including transport parameters for

occluded skin, may be found in Bhatt et al. (2008) and Nitsche and Kasting (2008). The key paper for understanding the stratum corneum component of the model is Wang et al. (2007), and the corresponding paper for dermis is Kretsos et al. (2008). At the present time, viable epidermis is treated as unperfused dermis. Each skin layer i in the diffusion model is represented by a slab having diffusivity D_i, partition coefficient K_i, and thickness h_i. All partition coefficients are expressed relative to the unionized form of the permeant in water. The upper SC has a porous deposition region of thickness h_{dep} into which topically applied compounds are immediately deposited. The value of h_{dep} is 10% of the SC thickness, h_{sc}. For volatile compounds, there is a first-order surface loss that may be represented by a gas-phase mass transfer coefficient k_g. The value of k_g depends on molecular weight and wind velocity, u, as described in Kasting and Miller (2006).

In addition to diffusion and evaporation, there is an option for permeant loss within each layer of the skin due to chemical degradation, metabolism, binding, etc. Losses are represented by first-order rate constants, k_i, where i represents the tissue layer. The loss rate is calculated as $k_i C_i$, where C_i is the local concentration of permeant in the tissue. For example, capillary clearance in the dermis is represented by a first-order rate constant k_{de}, which is turned on when analyzing *in vivo* absorption and set to zero for *in vitro* studies. The k_{de} value employed for models 2 and 3 in the present analysis is an additional clearance representing binding of parathion to dermis tissue. For the present analysis, k_{ed} was set equal to k_{de} and k_{sc} was set equal to zero. Thus, losses due to tissue binding were assumed to occur only in the viable skin layers.

Parameters derivable from the above information are reported in Tables 4 and 5. They include the saturation concentration of permeant in the SC (C_{sat}), the saturation dose of permeant in the deposition layer (M_{sat}), the steady-state skin permeability coefficient (k_p), and the volatility parameter (χ). Formulas for these parameters are given here:

$$C_{sat} = K_{sc} S_w \tag{A-1}$$

$$M_{sat} = C_{sat} \times h_{dep} \tag{A-2}$$

$$k_g = 6320\, u^{0.78} / MW^{1/3} \tag{A-3}$$

$$k_{evap}\rho = k_g \frac{P_{vp} MW}{7.6 \times 10^5 RT} \tag{A-4}$$

$$\chi = \frac{h k_{evap} \rho}{D C_{sat}} \tag{A-5}$$

REFERENCES

Agricultural Research Service 2009. *ARS pesticide properties database*. U.S. Department of Agriculture [accessed January 15, 2009]. http://www.ars.usda.gov/Services/docs.htm?docid=14147.

Bartek, M. J., and LaBudde, J. A. 1975. Percutaneous absorption in vitro. In *Animal models in dermatology*, ed. H. I. Maibach, pp. 103–120. Edinburgh: Churchill-Livingstone.

Bhatt, V. D., Soman, R. S., Miller, M. A., and Kasting, G. B. 2008. Permeation of tecnazene through human skin in vitro as assessed by HS-SPME and GC-MS. *Environ. Sci. Technol.* 42:6587–6592.

Bronaugh, R. L., and Stewart, R. F. 1984. Methods for in vitro percutaneous absorption studies III: Hydrophobic compounds. *J. Pharm. Sci.* 73:1255–1258.

Bucks, D. A. W., Hinz, R. S., Sarason, R., Maibach, H. I., and Guy, R. H. 1990. In-vivo percutaneous absorption of chemicals in a multiple dose study in rhesus monkeys. *Food Chem. Toxicol.* 28:129–132.

Chang, S. K., and Riviere, J. E. 1991. Percutaneous absorption of parathion in vitro in porcine skin: Effects of dose, temperature, humidity and perfusate composition on absorptive flux. *Fundam. Appl. Toxicol.* 17:494–504.

Chang, S. K., and Riviere, J. E. 1993. Effect of humidity and occlusion on the percutaneous

absorption of parathion in vitro. *Pharm. Res.* 10:152–155.

Chang, S. K., Williams, P. L., Dauterman, W. C., and Riviere, J. E. 1994. Percutaneoous absorption, dermatopharmacokinetics and related biotransformation studies of carbaryl, lindane, malathion and parathion in isolated perfused porcine skin. *Toxicology* 91:269–280.

Farahmand, S., and Maibach, H. I. 2009. Estimating skin permeability from physicochemical characteristics of drugs: A comparison between conventional models and an in vivo-based approach. *Int. J. Pharm.* 375:41–47.

Feldmann, R. J., and Maibach, H. I. 1967. Regional variations in percutaneous penetration of ^{14}C-cortisol in man. *J. Invest. Dermatol.* 48:181–183.

Feldmann, R. J., and Maibach, H. I. 1969. Percutaneous penetration of steroids in man. *J. Invest. Dermatol.* 52:89–94.

Feldmann, R. J., and Maibach, H. I. 1970. Absorption of some organic compounds through the skin in man. *J. Invest. Dermatol.* 54:399–404.

Feldmann, R. J., and Maibach, H. I. 1974. Percutaneous penetration of some pesticides and herbicides in man. *Toxicol. Appl. Pharmacol.* 28:126–132.

Fredriksson, T. 1961. Studies on the percutaneous absorption of parathion and paraoxon II. Distribution of ^{32}P-labelled parathion within the skin. *Acta Derm. Venereol.* 41:344–352.

Hawkins, G. S., and Reifenrath, W. G. 1984. Development of an in vitro model for determining the fate of chemicals applied to skin. *Fundam. Appl. Toxicol.* 4:S133–S144.

Integrated Chemical Management Solutions. 2009. *ChemGold MSDS*. [accessed January 15 2009]. http://ucinc.chemwatchna.com

Kasting, G. B., Filloon, T. G., Francis, W. R., and Meredith, M. P. 1994. Improving the sensitivity of in vitro skin penetration experiments. *Pharmaceut. Res.* 11:1747–1754.

Kasting, G. B., Francis, W. R., Bowman, L. A., Kinnet, G. O. 1997. Percutaneous absorption of vanilloids: In vivo and in vitro studies. *J. Pharm. Sci.* 86:142–146.

Kasting, G. B., Miller, M. M., and Talreja, P. S. 2005. Evaluation of stratum corneum heterogeneity. In *Percutaneous absorption,* eds. R. L. Bronaugh and H. I. Maibach, pp. 193–212. New York: Taylor & Francis.

Kasting, G. B., and Miller, M. A. 2006. Kinetics of finite dose absorption through skin 2. Volatile compounds. *J. Pharm. Sci.* 95:268–280.

Kasting, G. B., Miller, M. A., and Bhatt, V. 2008a. A spreadsheet-based method for estimating the skin disposition of volatile compounds: Application to *N,N*-diethyl-*m*-toluamide (DEET). *J. Occup. Environ. Hyg.* 10: 633–644.

Kasting, G. B., Miller, M. A., and Nitsche, J. M. 2008b. Absorption and evaporation of volatile compounds applied to skin. In *Dermatologic, cosmeceutic and cosmetic development*, eds. K. A. Walters and M. S. Roberts, pp. 385–400. New York: Informa Healthcare USA.

Kim, Y. H., Woodrow, J. E., and Seiber, J. N. 1984. Evaluation of a gas chromatographic method for calculating vapor pressures with organophosphorus pesticides. *J. Chromatogr.* 314:37–54.

Kim, Y. H., Ghanem, A. H., Mahmoud, H., and Higuchi, W. I. 1992. Short chain alkanols as transport enhancers for lipophilic and polar ionic permeants in hairless mouse skin. *Int. J. Pharm.* 80:17–31.

Kretsos, K., and Kasting, G. B. 2007. A geometrical model of dermal capillary clearance. *Math. Biosci.* 208:430–453.

Kretsos, K., Miller, M. A., Zamora-Estrada, G., and Kasting, G. B. 2008. Partitioning, diffusivity and clearance of skin permeants in mammalian dermis. *Int. J. Pharm.* 346: 64–79.

Maibach, H. I., and Feldmann, R. J. 1974. Systemic absorption of pesticides through the skin of man. In *Occupational exposure to pesticides: Report to the Federal Working Group on Pest Management from the Task Group on Occupational Exposure to Pesticides*, Appendix B. Washington, DC: U.S. Government Printing Office.

Maibach, H. I., Feldmann, R. J., Milby, T. H., and Serat, W. F. 1971. Regional variations in

percutaneous penetration in man. *Arch. Environ. Health* 23:208–211.

Merritt, E. W., and Cooper, E. R. 1984. Diffusion apparatus for skin penetration. *J. Controlled Release* 1:161–162.

Miller, M. A., Bhatt, V., Kasting, G. B. 2006. Absorption and evaporation of benzyl alcohol from skin. *J. Pharm. Sci.* 95:281–291.

Moody, R. P., Akram, M., Dickson, E., and Chu, I. 2007. In vitro dermal absorption of methyl salicylate, ethyl parathion, and malathion: First responder study. *J. Toxicol. Environ. Health A* 70:985–999.

Ngeh-Ngwainbi, J., Foley, P. H., Kuan, S. S., and Guilbault, G. G. 1986. Parathion antibodies on piezoelectric crystals. *J. Am. Chem. Soc.* 108: 5444–5447.

Nitsche, J. M., Wang, T.-F., and Kasting, G. B. 2006. A two-phase analysis of solute partitioning into the stratum corneum. *J. Pharm. Sci.* 95: 649–666.

Nitsche, J. M., and Kasting, G. B. 2008. Biophysical models for skin transport and absorption. In *Dermal absorption and toxicity assessment*, eds. M. S. Roberts and K. A. Walters, pp. 249–267. New York: Informa Healthcare USA.

Nolan, R. J., Rick, D. L., Freshour, M. L., and Saunders, J. H. 1984. Chlorpyrifos: Pharmacokinetics in human volunteers. *Toxicol. Appl. Pharmacol.* 73:8–15.

Organization for Economic and Community Development. 2004. *Guidance document on dermal absorption*. Geneva: OECD.

Organization for Economic and Community Development. 2004. *Skin absorption: In vitro method*. Organization for Economic and Community Development Guidelines 428. Geneva: OECD.

Qiao, G. L., Chang, S. K., and Riviere, J. E. 1993. Effects of anatomical site and occlusion on the percutaneous absorption and residue pattern of 2,6-(ring-carbon-14) parathion in vivo in pigs. *Toxicol. Appl. Pharmacol.* 122: 131–138.

Qiao, G. L., and Riviere, J. E. 1995. Significant effects of application site and occlusion on the pattern of cutaneous penetration and biotransformation of parathion in vivo in swine. *J. Pharm. Sci.* 84: 425–432.

Qiao, G. L., Williams, P. L., and Riviere, J. E. 1994. Percutaneous absorption, biotransformation, and systemic disposition of parathion in vivo in swine. *Drug Metab. Dispos.* 22:459–471.

Ray Chaudhuri, S., Gajjar, R. M., Krantz, W. B., and Kasting, G. B. 2009. Percutaneous absorption of volatile solvents following transient liquid exposures. II. Ethanol. *Chem. Eng. Sci.* 64:1665–1672.

Reifenrath, W. G. 1995. Volatile substances. *Cosmet. Toilet.* 110:85–92.

Reifenrath, W. G., and Hawkins, G. S. 1986. The weanling Yorkshire pig as an animal model for measuring percutaneous penetration. In *Swine in biomedical research*, ed. M. E. Tumbleson, pp. 673–680. New York: Plenum Press.

Reifenrath, W. G., Hawkins, G. S., and Kurtz, M. S. 1991. Percutaneous penetration and skin retention of topically applied compounds: An in vitro-in vivo study. *J. Pharm. Sci.* 80:526–532.

Santhanam, A., Miller, M. A. and Kasting, G. B. 2005. Absorption and evaporation of *N,N*-diethyl-*m*-toluamide (DEET) from human skin in vitro. *Toxicol. Appl. Pharmacol.* 204:81–90.

Shah, P. V., and Guthrie, F. E. 1983. Percutaneous penetration of 3 insecticides in rats: A comparison of 2 methods for in-vivo dermination. *J. Invest. Dermatol* 80: 291–293.

U.S. Environmental Protection Agency. 2009. Estimation Programs Interface Suite™ for Microsoft® Windows 4.00. Washington, DC. http://www.epa. gov/oppt/exposure/pubs/episuite.htm

Van der Merwe, D., Brooks, J. D., and Riviere, J. E. 2006. A physiologically based pharmacokinetic model of organophosphate dermal absorption. *Toxicol. Sci.* 89:188–204.

van der Merwe, D., and Riviere, J. E. 2005. Effect of vehicles and sodium lauryl sulfate on xenobiotic permeability and stratum corneum partitioning in porcine skin. *Toxicology* 206:325–335.

Wang, T.-F., Kasting, G. B., and Nitsche, J. M. 2006. A multiphase microscopic model for stratum corneum permeability. I. Formulation, solution and illustrative results for representative compounds. *J. Pharm. Sci.* 95:620–648.

Wang, T.-F., Kasting, G. B., and Nitsche, J. M. 2007. A multiphase microscopic model for stratum corneum permeability. II. Estimation of physicochemical parameters and application to a large permeability database. *J. Pharm. Sci.* 96:3024–3051.

Wester, R. C., and Maibach, H. I. 1976. Relationship of topical dose and percutaneous absorption in rhesus monkey and man. *J. Invest. Dermatol.* 67:518–520.

Wester, R. C., and Maibach, H. I. 1985. In vivo percutaneous absorption and decontamination of pesticides in humans. *J. Toxicol. Environ. Health* 16:25–37.

Wester, R. C., Melendres, J. L., and Maibach, H. I. 1996. In vivo percutaneous absorption of acetochlor in the rhesus monkey: Dose-response and exposure risk assessment. *Food Chem. Toxicol.* 34: 979–983.

Wester, R. M., Tanojo, H., Maibach, H. I., and Wester, R. C. 2000. Predicted chemical warfare agent VX toxicity to uniformed soldier using parathion in vitro human skin exposure and absorption. *Toxicol. Appl. Pharmacol.* 168:149–152.

Yamashita, F., Yoshioka, T., Koyama, Y., Okamoto, H., Sezaki, H., and Hashida, M. 1993. Analysis of skin penetration enhancement based on a 2-layer skin diffusion model with polar and nonpolar routes in the stratum corneum. *Biol. Pharm. Bull.* 16:690–697.

Zhai, H., and Maibach, H. I. 2001. Effects of skin occlusion on percutaneous absorption: an overview. *Skin Pharmacol. Appl. Physiol.* 14:1–10.